Results from an LHC-structured beamtest of SCT prototype modules

A.Barr [a], M.Donega [e], M.D'Onofrio [e], L.Eklund [b],
J.E.Garcia Navarro [h], P.Kodys [c], G.F.Moorhead [f], P.Phillips [g]
P.Reznicek [b], M.Vos [h], R.Wallny [b]

[a] *University of Cambridge, England*
[b] *CERN*
[c] *Charles University, Prague, Czech Republic*
[d] *Czech Technical University, Prague, Czech Republic*
[e] *University of Geneva, Switzerland*
[f] *University of Melbourne, Australia*
[g] *Rutherford Appleton Laboratory, UK*
[h] *IFIC, University of Valencia, Spain*

Abstract

A beam with an LHC-like time structure, very short bunches of particles at 25 ns spacing, was available from the CERN SPS during October 2001. This beam was used at the ATLAS H8 testbeam facility to measure on non-irradiated and irradiated SCT prototype modules effects related to the detailed timing of the readout. Four SCT modules were arranged to form a binary telescope, allowing high readout rates, relatively high beam intensities and providing a time stamp for the reconstructed tracks with reasonable spatial resolution. We report the most important results in this note.

1 Introduction

In the October 2001 test beam period, the SPS was operated with a time structure similar to the envisaged bunch crossing structure of the LHC. The readout of the SCT modules - including the ABCD front-end chips - used the same clock as the accelerator, provided by the LHC TTC system to the ATLAS H8 barracks. This ensured synchronicity of particle arrival in the detector and sampling of the resulting signal. In this note we report on a number of specific studies of the performance of SCT modules that were made possible by the

availability of the structured beam. In sections 2 and 3 the modules under test and the specific setup for this beam test and are briefly introduced.

During the beam test four SCT barrel module prototypes were arranged and configured to act as a binary telescope. The use of detectors with SCT electronics, with fast shaping and pipelined, buffered readout, allowed tests at much higher beam intensities and trigger rates than is possible with the Viking/VA2 chips of the standard analogue telescope normally used for SCT beamtests, albeit at lower spatial resolution. The binary telescope thus allowed an unambiguous time stamp to be assigned to tracks. Results on the time and spatial resolution of this binary tracking array are reported in section 4.

Some preprocessing is done on the raw data to facilitate analysis by the SCT community. This includes the alignment of the telescope and modules-under-test system and the reconstruction of the tracks of the beam particles. The availability of these DSTs of preprocessed data and related analysis software is briefly described in section 5.

During most of the LHC-like beam period, the beam intensity was relatively low. Furthermore, the DAQ was configured for single-event readout, the operating mode used in the more usual asynchronous SCT beamtests, such that each event was completely read out after a trigger from the scintillators before the veto was released for a further trigger. The resulting dead time, together with the low beam intensity, makes this study insensitive to effects due to pile up of events. The main measurement programme in this period consisted of a scan of the delay between the accelerator clock and the readout clock. This allowed an explicit mapping of the tracking performance of the modules as a function of time. On the one hand this provides an important cross check to some of the timing studies done using asynchronous beam tests. On the other hand, studies of intricate timing effects that cannot be studied normally become possible due to the tight, well known timing of the particle arrival. The results of this study are reported in section 6.

In the second part of the beamtest, the beam intensity was raised to check the effects of the high intensity on module resolution. For the highest beam intensities the probability to have two tracks closely spaced in time is quite high. A special 'dead-time free' mode of readout '8L1' was devised to be able to read-out eight consecutive events. This allows us to study effects on the performance of the modules of tracks crossing the modules inmediately previous to the event. Section 7 reports on these studies and will present a measurement of the double pulse resolution.

Results from the asynchronous beam tests in August and October 2001 are reported elsewhere [1]. More information on SCT beamtests can be found in notes from previous years [3–5]. For a detailed introduction to the SCT

Slot	*Name*	*Type*	*Irradiated?*	*Hybrid*	*Chips*	*T (°C)*
Y0	K3112	Barrel		B K?	2T	+4
0	0035	Barrel		B K4	3TA	-4
1	0046	Barrel		B K4	3TA New-epi	-7
2	0052	Barrel		B K5	3TA New-epi	-6
3	0047	Barrel	*	B K4	3TA New-epi	-8
4	0044	Barrel	*	B K4	3TA New-epi	-10
5	0029	Barrel		B K4	3TA	-8
6	0048	EC "KB"		B K4	3TA	-3
7	K4_211	EC Middle		E K4	3TA	+5
8	(vacant)					
9	0036	Barrel		B K4	3TA	-9
Y1	K3104	Barrel		B K?	2T	+3

Table 1
Modules in the October beamtest. In this beamtest, four modules were used to form a binary telescope. The first and last standard positions, 0 and 9, were occupied by two modules measuring the X coordinate, and two new positions upstream and downstream of these were occupied by modules placed at right-angles measuring the Y position (in notional slots labelled Y0 and Y1.) The other modules were all under test. The modules are spaced at a 45 mm pitch.

detector the reader is referred to [6,8].

2 Modules tested

The modules tested in October 2001 are summarised in table 1. Five were barrel modules built for the Barrel FDR/PRR, four of which used ABCD3TA chips from wafers with an epitaxial layer supplied by a new vendor. One module with old-epi chips tested in August, 0029, was included to act as a control sample. Two prototype end-cap modules were also present, one of them built with a barrel hybrid and the other with a K4 hybrid. To complete the setup, four additional barrel modules were included arranged to form the binary telescope. Two of these were recent modules with ABCD3TA chips, and two were older modules with ABCD2T chips.

3 Setup

The ATLAS SCT beamtest setup at the H8 beamline at the CERN SPS in October 2001 was described in some detail in the note that reports on the standard measurements performed in the 2001 beamtests [1]. Apart from the beam, the main difference with the standard beam test procedure was that the analog telescope was not used. The experience and results from a "binary telescope", made of SCT modules, are reported in a dedicated section 4 where some changes in the setup specific to the synchronous beam measurements are briefly discussed.

During the October beamtest the SPS had a special bunch structure which was similar in some respects to that intended for the LHC for which the SPS will be the injector. The protons in the SPS were bunched in narrow groups of about 1 ns length, spaced at 25 ns corresponding to the 40 MHz RF. This bunch structure was interrupted into trains of around 70 cycles synchronised to the 43 kHz orbital frequency in the SPS. The secondary pions arriving in the H8 beamline at the detector preserved this structure, although with a rather low occupancy probability in each bunch (less than 1.0). This had the effect that particles arrived only at integer multiples of the 25 ns clock period.

The 40 MHz bunch clock as well as the 43 kHz beam orbit clock signals were both available from the accelerator controls via the LHC TTC system to the ATLAS H8 barrack where they were converted to NIM levels used in the SCT trigger and control logic. The global 40 MHz clock was used to drive the SCT system via the External Clock input of the CLOAC Clock and Control module and distributed to the detector modules by SLOG slow command generators in the usual way. This assured synchronicity, up to an arbitrary phase delay, of the readout clock with the signal deposition in the silicon detectors. The clock phase delay was controlled and adjusted by cable delays.

The electronic signals related to the bunch structure are depicted schematically in figure 1. The synchronous 43 kHz beam orbit signal was used to trigger the sending of a Bunch Crossing Counter (BC) Reset command to the module front-end ASICs (fourth trace) using the CLOAC External BC Reset input. The particle bunch train then followed after a certain fixed delay. Each coincidence from the trigger scintillators associated with a particle passage was used to generate the sending by CLOAC of Level 1 Accepts (L1As) after an additional fixed delay (108 clocks) to compensate for the ABCD chip pipeline (third trace.) The number of clock cycles (bunch crossings) and the number of L1As since the last BC Reset are counted in the ABCD chips and are included in the ABCD data header for each event. This information can be used offline to create a time stamp for the event and thus ensure synchronicity of the DUT and binary telescope readout.

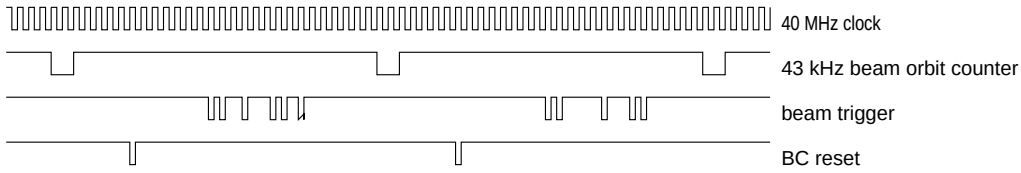

Fig. 1.

In asynchronous beam tests, without the structured beam, the random delay between the arrival of the particle (the trigger signal from the scintillators) and the clock is routinely measured with a Time to Digital Converter. This information is used offline to select a time interval where the electronics samples the peak of the shaper pulse. In perfectly synchronous running this measurement would be expected to give a delta peak. Figure 3 contrasts the measured TDC distribution from standard asynchronous 2(a) tests and the present synchronous 2(b) operation. The distribution for the synchronous operation 2(b) shows the expected narrow peak. The width of the peak, resulting from the combined clock and trigger jitter, is of the order of 100s of picoseconds. Differences in the measured center of the peak for different cable delays can be used as a cross check of these delays. During some time of the beam period, the accelerator experienced problems with the High Voltage of the RF chambers. This resulted in a wider distribution with side-peaks at intervals of integer multiples of the period of the RF chamber (160 MHz). These side-peaks could effectively be removed offline by requiring the TDC value to fall in a narrow region around the center of the peak.

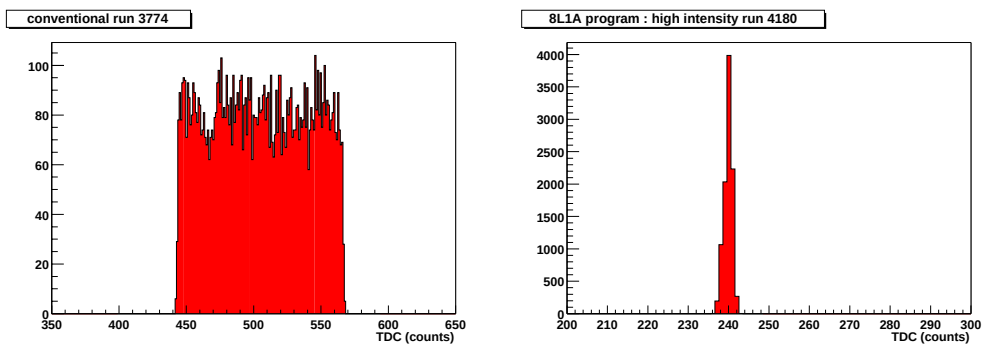

(a) (b)

Fig. 2. Distributions of the measurement of the delay between the scintillator trigger and the system clock. A TDC count corresponds to 0.2 ns. *(a)*: Asynchronous beam and *(b)* synchronous beam

In order to be able to measure the effects of high beam intensity some changes had to be made to the setup between the first part of the programme and the dedicated high intensity runs. Most importantly, the CLOAC settings were altered so that on arrival of a raw trigger, after a delay of an integer number

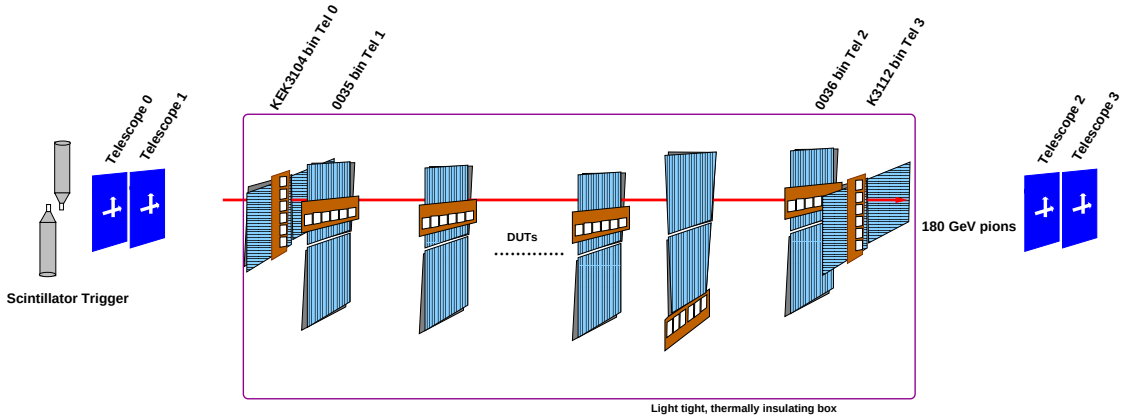

Fig. 3. A sketch of the layout of the beamline in October 2001. Four modules - two horizontal and two vertical - make up the binary telescope. All modules under test were placed vertically.

of clock cycles, instead of just one L1A, eight consecutive L1A signals (i.e., the digital chain $110110\ldots110$) were issued to the modules. As the ABCD chip is designed to return occupancy data from three consecutive timebins for each L1A pattern (110), this procedure resulted in the full binary information from an interval of $8 \times 3 \times 25 = 600$ nanoseconds being obtained.

4 The binary telescope

The required trigger rates and beam intensities in the October beam test were prohibitive for the slow analogue telescope normally used to reconstruct tracks. Therefore, in addition to the modules under test, four standard SCT barrel modules were read out throughout the beamtest. These were used to form a 'binary telescope', mounted in X-Y pairs in the most upstream and downstream positions available. The X modules were in the outermost standard slots, whereas the Y modules were mounted in newly arranged horizontal positions to measure the vertical (Y) coordinate, see figure 3. These modules did not participate in threshold scans but were kept at a fixed threshold of 1.2fC for reasonable efficiency and low noise. Two of the modules were from those tested in August, and two, with ABCD2T chips, from those tested in 2000.

Tracks are reconstructed from the hit information in the binary telescope. Hits are combined in four pairs of X and Y planes to make up three dimensional space points. A track finding algorithm then uses combinations of points on opposite sides of the system to define straight tracks. Only when four XY points line up is the track accepted.

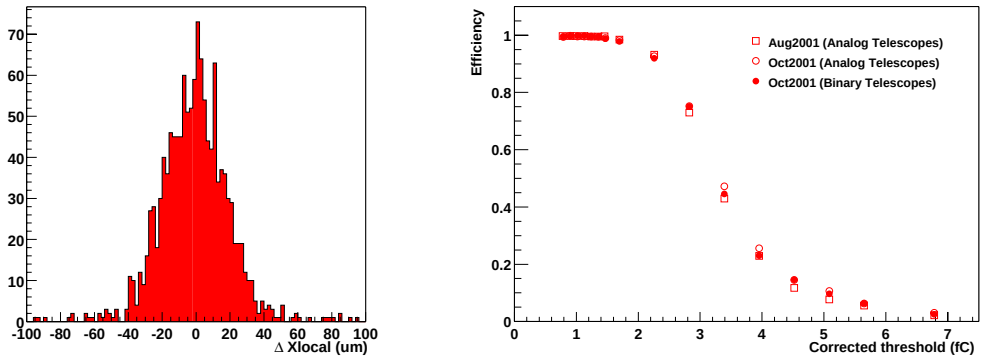

(a) (b)

Fig. 4. a) The difference between the prediction of analog and binary telescopes for the X coordenate of the track in the local reference system of an example module (number 6, link 0.) b) Efficiency versus threshold obtained from three analyses using different telescopes for the track reconstruction.

The SCT modules used in the binary telescope have virtually no dead regions. Therefore, the track reconstruction effiency is very high: for 90 % of the scintillator triggers at least one track was successfully reconstructed.

4.1 Spatial resolution

The spatial resolution of SCT modules is approximately 23 microns, whereas that of the VA2 telescope modules is around 5 microns. Therefore, one expects the track extrapolation precision to become worse when moving from the analog to the binary telescope.

In order to study this effect, tracks were reconstructed by both methods in a run where both telescopes were read out. Figure 4 compares the prediction of the track position by both telescopes. To a good approximation, the error on the analogue prediction can be ignored. The track interpolation precision of the binary telescope is thus equal to the root mean square of the distribution: 17 microns.

Even though the precision of the track position prediction is significantly worse than with the analog system and no longer small compared to the resolution of the devices under test, for most studies the obtained precision is sufficient. Over 92 % of the tracks reconstructed with the binary telescope correctly identify the strip the particle traversed, sufficient information for the definition of efficiency.

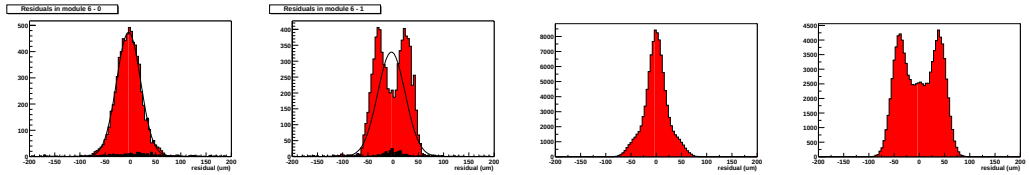

(a) (b) (c) (d)

Fig. 5. Residuals: the difference between the prediction of the binary telescope and the measurement of module 6 link 0 (a) and link 1 (b). Residuals obtained from a simple geometrical simulation: (c) perfectly aligned modules and (d) the module under test is offset by 40 microns.

Figure 4(b) compares the efficiency vs threshold result obtained from an analysis using the tracks reconstructed from the information in the binary and analog telescopes. The squares were obtained from an analysis of August data, with a VIKING analogue telescope. The circles correspond to a series of runs with asynchronous readout that were taken in October to enable comparison to standard beam tests. In these runs two telescopes were read out simultaneously: a VA2 telescope similar to that in August and the binary telescope. No systematic differences are observed between the three sets of results.

4.2 Effects of binary readout

The discrete nature of the binary readout is known to distort the shape of the difference of two position measurements. Its effect on the alignment scheme for ATLAS has been simulated in some detail [9]. In the case of the binary telescope the residuals are the difference between the track position predicted by the telescope and the position measured by the module under test. As the track prediction is based on a limited number (4) of discrete position measurements, these distortions occur - to a lesser extent - when constructing the residuals in the binary telescope.

The residual distributions of two planes of the same module are shown in figure 5 (a and b). Link 0 of module 6 shows a rather narrow, non-Gaussian distribution, whereas link 1 of the same module has a typical double peak structure.

These shapes can be reproduced qualitatively by a simple geometrical simulation. It takes into account the uniform spatial distribution of the beam particles and generates an angular distribution close to the one observed in the beamtest. The position measured by the module is simply the closest integer multiple of the pitch. The track reconstructed by the binary telescope is simply the line joining the two telescope modules up- and downstream of the

module under test. The distributions in figure 5 (c and d) present the model prediction for the residuals in the cases the three modules are perfectly aligned (c) and offset by half a pitch (d).

4.3 Time resolution

For the high intensity studies the possibility to time-stamp the track (i.e., identify the clock cycle that the particle traversed the setup) is of crucial importance. As the beam is synchronous, identification of the clock cycle provides the full time information for the track. In the ABCD3TA chips, an L1A trigger causes the binary hit information of three consecutive cells in the trigger latency pipeline, corresponding to the discriminator output of three samples separated by 25 ns, to be read out. During the beamtest, the modules are read out in ANYHIT data compression mode so that none of this hit information is lost in the read out process. For the high intensity program the timing sensitivity of the modules is increased by operating the discriminator in Edge Sensing mode [1].

The track finding algorithm uses hits from one single time bin to reconstruct the tracks. An exception is made for the two ABCD2T modules that were not very well synchronized to the rest of the system: in these modules hits are accepted from the current and next time bin. The smearing of the time information on a limited number of modules does not lead to a significant deterioration of the resolution of the track time stamp.

5 DST production

After offline processing, test beam data are made available to the community in the form of DSTs. These contain all relevant data in an easily accessible format (a ROOT TTree). Most importantly, the internal alignment of the telescope to the modules under test is available in the form of alignment files. The iterative algorithm that obtains the alignment from the hit information in the modules has been described elsewhere [4,1]. In the October test beam, dedicated alignment runs, where the analogue telescope modules were also read out, were taken whenever necessary. Thus, the standard procedure could be used and the alignment benefits from the high spatial resolution of the analog telescope modules.

[1] The Edge Sensing circuit issues a 25 ns long high on the rising edge of a signal crossing the threshold. The effect is that exactly one binary '1' is loaded into the pipeline, even if the pulse remains over threshold during several clock cycles

The offline also reconstructs tracks from the telescope information which is stored with each event. Furthermore, consistency of the data with, for example, the ABCD protocol, is checked to catch readout errors. The standard format of the DST has been modified slightly to incorporate the time information of the tracks and the possibility of multiple triggers in one event. DSTs are available in the form of ROOT files on the CERN tape storage system CASTOR [10]. Alignment files, software libraries of the new format DSTs and some examples of analysis macros can be found on the offline web pages [11].

6 Low intensity programme

During most of the October test program one event was read out for each scintillator trigger coincidence. The readout is synchronous, i.e., the delay between signal deposition and sampling is fixed. Adding or removing fixed lengths of cabl in the external clock line varies this delay. The low intensity programme consisted of a scan of the cable delay in steps of 2.75 ns. For each delay a full threshold scan was taken.

Figure 6(a) shows the resulting S-curves for a number of delays. The amplitude of the signal depends strongly on the sampling delay. Combining median charge measurements for all delays, the shaper pulse can be reconstructed [2], see figure 6(b). The four delays for which the S-curves were shown in figure 6(a) are indicated with red markers in figure 6(b).

The charge result for the optimum cable delay can be used to cross check the standard test beam charge determination. In asynchronous operation the sampling time is uniformly distributed in the 25 ns interval. Events with a delay outside an optimized time window are rejected. Thus the efficiency is the average value over the width of a 10 ns window around the central part of Figure 6(b), while in the synchronous case it is tuned to read the pulse at the maximum. Figure 7 shows two s-curves for the same module. One of them corresponds to synchronous readout for the optimal value of the delay and the other to asynchronous readout. The variation of points position from one to another is minimal, but the efficiency in the synchronous case is a bit higher.

Table 2 is a summary of the charge results for barrel modules [3]. The first two columns correspond to the same, asynchronous run. The first was analysed

[2] On an L1A trigger, the ABCD chip releases binary information from three clock cycles. This property is used to extend the range of the scan to the full 75 ns of the figure

[3] All the values of charge shown are corrected by a multiplicative factor of 1.13 corresponding to the global batch calibration.

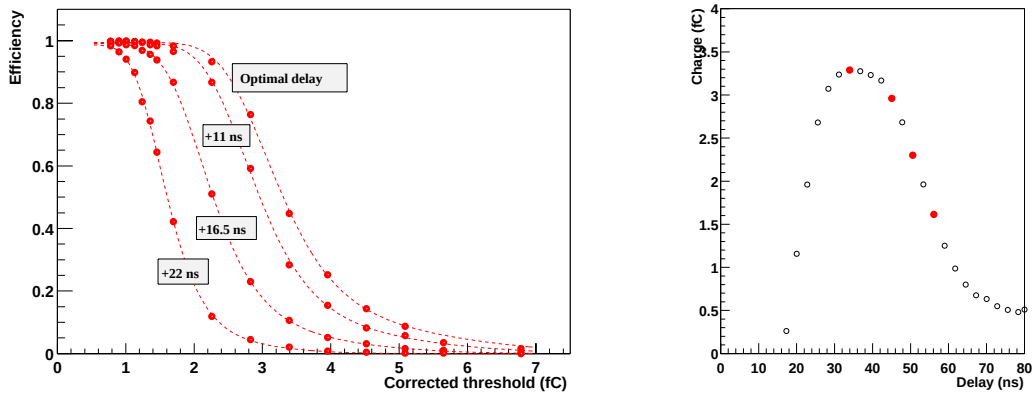

(a) (b)

Fig. 6. S-curves from data taken with synchronous readout with different delays between beam clock and trigger, left. Position of the data represented by the s-curves in the pulse shape, dark markers, right.

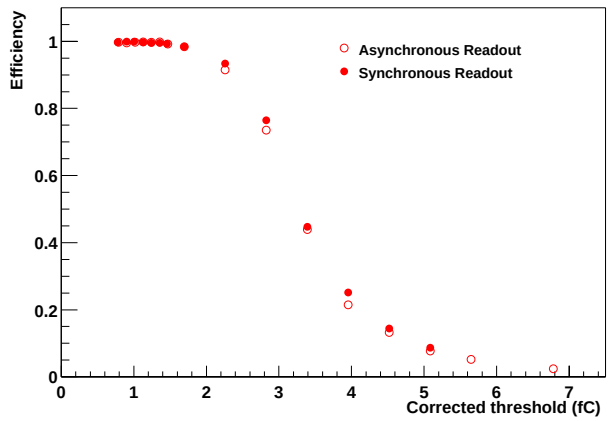

Fig. 7. Two s-curves of the same module from data of an asynchronous run, white markers, and synchronous run, dark markers.

using the analog telescope, while in the second the binary telescope is used to reconstruct the tracks. The third column is the charge result for a synchronous run. The sampling delay has been optimised separately for each module.

Three main factors contribute to the inaccuracy of the value of the median charge: minimum step of the threshold DAC, error in the calibration of the calibration DAC, and error on the fit. The threshold DAC step is 2.5 mV corresponding to 0.05 fC. The calibration DAC error is around 2.5% [12], or equivalent in charge 0.08 fC. Finally, the error made fitting data to the s-curve function is around 0.02 fC (depending on the number of points). Adding all the

Module	Analog Telescopes	Binary Telescopes	Synchronous Readout
0046	3.31	3.27	3.23
0052	3.37	3.39	3.45
0047*	3.10	3.13	3.16
0044*	3.07	3.09	3.16
0048	3.28	3.29	3.18

Table 2
Median charge obtained with different methods: asynchronous runs analysed using the analog and binary telescope and a synchronous readout run with binary telescope.

contributions quadratically the error is ± 0.09 fC [4] Within this error, results for all methods are compatible.

Another test is the comparison between the reconstructed pulse shape of the chip with asynchronous and synchronous data. The methods for reconstructing the pulse shape are quite different. For the asynchronous pulse shape the arrival time of the particles is measured with the TDC [1]. In the synchronous pulse shape (Figure 6(b)), the delay is varied explicitly by the delay in the external clock line as explained above.

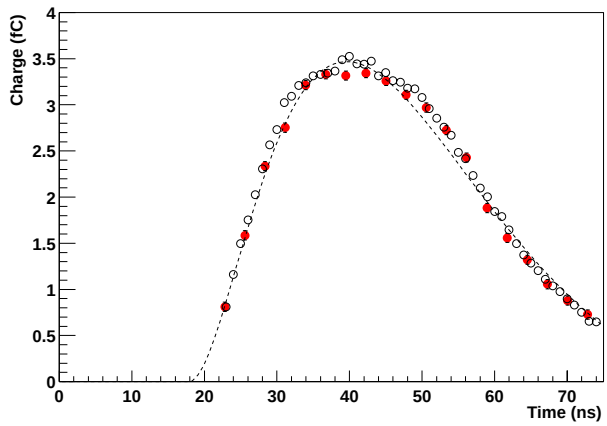

Fig. 8. Pulse shapes for a non irradiated barrel module 0046: white markers, the asynchronous data; dark markers, the synchronous data.

Figure 8 shows two pulse shapes for a non-irradiated barrel module. The asynchronous data is represented with white markers, dark markers correspond to

[4] Measurements in the May 2002 test beam confirm this argument.

the synchronous data. The offset of the time scale depends on the setup and has been adjusted offline to overlay both pulses. The vertical scale shows median charges obtained from s-curves for the different delays. No data with less than 0.7 fC has been plotted because this is the lowest threshold measured in the beamtest and extrapolation to lower value is not very accurate. Both methods yield a very similar pulse shape. The peaking time can be obtained by fitting the ABCD function to the pulse shapes[13], Table3 compares the peaking time results of synchronous and asyncronous pulse shape reconstruction for the different links of five modules.

Module	link	Peaking time (ns)	
		Asynchronous	Synchronous
0046	link 0	21.7	21.8
	link 1	22.6	22.7
0052	link 0	19.4	20.8
	link 1	20.1	20.8
0047*	link 0	23.4	23.5
	link 1	24.8	24.7
0044*	link 0	23.2	22.6
	link 1	23.3	23.5
0048	link 0	21.7	22.0

Table 3
Peaking times of five modules present in the October test beam. Results are given separately for each link. The first column corresponds to asynchronous, the second to synchronous readout.

The resulting peaking times are very similar. The largest differences are of the order of nanoseconds. As it was seen in [1], the variation between modules is around $\pm$ 0.6 ns, corresponding to the change batch to batch for non-irradiated modules and a little higher, $\pm$ 0.7 ns for irradiated modules. In the same batch chips have an error of peaking time that is $\pm$ 0.4 ns. Most values agree within this error.

6.1 Ghost hits

In the SCT detector design charge is mostly collected on a single strip. Some charge, however, is shared between two strips through dispersion of charge in the Silicon or cross talk due to the interstrip capacitance. At non-perpendicular

incidence, the projection of the charge deposition on the readout plane can become quite large and charge sharing becomes significant. Small charges due to charge sharing are likely to give a late discriminator response (time walk) and can thus appear in the next time bin.

The bunch crossing frequency of 40 MHz requires the front-end electronics to react very fast to the signal. The peaking time of the ABCD shaper is of the order of 20 ns. Signal spilling over into the next event can cause hits that are not related to any track in that event, so-called Ghost Hits (see Figure 9).

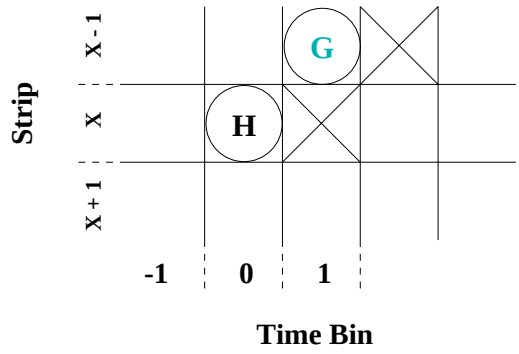

Fig. 9. Example of a ghost hit with the Edge Sensing discrimintor mode ON in the ABCD chip. A track is incident at time *0* in strip *X*. The hit corresponding to the track is marked with a H. A small signal (due to charge sharing or cross talk) causes a "ghost" hit in the adjacent strip *X - 1* in the next time bin (marked with G).

In the ABCD chips, two configurable mechanisms increase the time sensitivity of the readout, the discriminator Edge Sensing circuit and the readout Compression Mode. With its Edge Sensing circuit mode ON, the discriminator issues a 25 ns "high" signal on detection of a signal crossing the threshold in the active direction, resulting in only one "1" being written into the pipeline. The readout Compression Mode of the chips selects certain digital hit patterns. The most aggressive pattern, Edge compression *01X*, requires that there was no hit in the given strip in the clock cycle before the trigger. This compression mode is quite effective in preventing any signals spilling over into the next bin from causing a hit, but is limited to the one strip. Small signals in neighbouring channels that time walk into the next event form a source of ghost hits that cannot be reduced by this process.

The October test beam data were taken with the discrimintor Edge Sensing mode OFF and in the least aggressive readout compression mode, Anyhit compression *XXX*. Offline, the effect of the Edge Sensing circuit on the hit pattern is simulated [5] .

[5] The hit pattern does not provide the full analogue information. The simulation can therefore never be perfect. Its validity has been cross checked, comparing to test beam data taken with Edge Sensing ON.

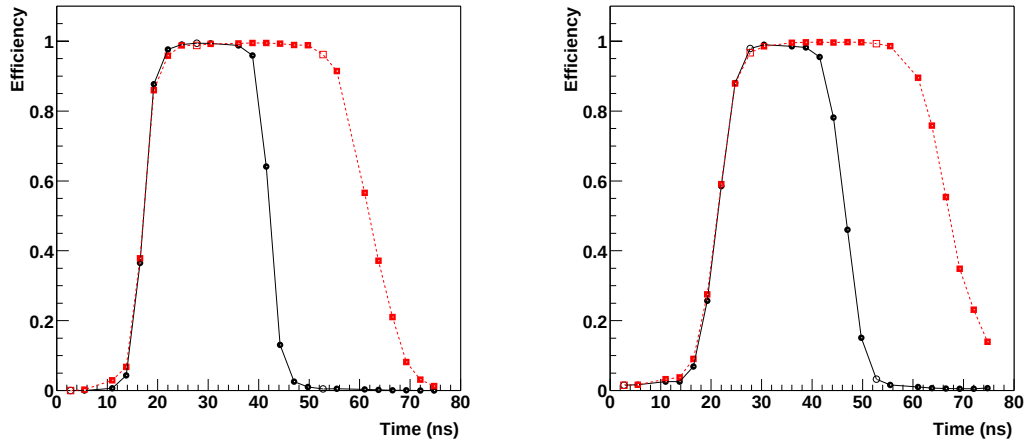

(a) (b)

Fig. 10. Variation of the efficiency with time for test beam data, squares, and after simulation of the Edge Sensing ON mode, circles, for a non irradiated module (a) and irradiated module (b)

The data from the nine delays used in the previous section has been taken for the simulation. Values of efficiency have been calculated for each of the delays and time bins. Figure 10 shows the variation with delay of the efficiency. The test beam results before application of the Edge Sensing simulation are shown with square, and the results after with round markers. Figure 10(a) corresponds to a non-irradiated module, figure 10(b) to an irradiated module. The effect of the Edge Sensing simulation on the tail of the signal is clear. A non zero "efficiency" due to irreducible ghost hits remains after applying the edge sensing algorithm.

For all modules, the optimum delay is chosen as the point in figure 10 with the highest efficiency. The resulting efficiency for optimum timing are listed in the first column in tabel 4. With the present statistics, the efficiency is compatible with 100% for the non-irradiated modules. It is consistently lower for the irradiated modules. This could be due to the higher noise or the increased time walk.

The second column lists the efficiencies at the points next to the optimum. This corresponds to a timing mismatch of 2.75 ns. The loss of efficiency due to a mismatch of the timing of 2.75 ns will cause a variation on the efficiency of less than 1 % in both cases.

As figure 10 covers an interval of 75 ns, the probability that a track leaves a ghost hit in the clock cycle after the trigger can also be estimated. The ghost hit probability corresponding to the optimum delay is the "efficiency"

	Optimum Efficiency (%)	Mismatch Efficiency (%)
Non-Irradiated	99.8 ± 0.2	99.5 ± 0.3
Irradiated	98.8 ± 0.5	98.0 ± 0.5

Table 4
Efficiencies at the optimum cable delay, and at the neighbouring cable delay in the scan, with a 2.75 ns mismatch.

of the point corresponding to a full clock cycle (25 ns) after the maximum. The results are given separately for non-irradiated and irradiated modules in table 5. The result is the mean value of all the links tested and the error is the standard deviation of the values.

As mentioned, two processes - charge sharing and cross talk - can induce the signal in adjacent strips that cause the ghost hits. One would expect that - at perpendicular incidence - the charge sharing is only significant in a narrow region between two strips. The relative weight of charge sharing and cross talk is evaluated by rejecting events where the hit prediction from the track extrapolation is in this region. A window of $\pm$ 12 μm has been left around the strip. The second column lists the ghost hit probability due to cross talk. For non-irradiated modules, charge sharing does not seem to contribute significantly to the ghost hits. In the irradiated modules at perpendicular incidence ghost hits due to cross talk form about two thirds of the total.

The probability to create a ghost hit is much larger in the irradiated modules than in non-irradiated modules of the same design. This effect can be produced by a number of factors. Of course, the noise in irradiated modules is higher. The shaper pulse becomes longer (this note and [1]). Finally, some authors[14] report an increase in the interstrip capacitance of ¡111¿ wafers after radiation.

Ghost hits can also be caused by real tracks. Therefore, the occupancy due to ghost hits in ATLAS is estimated as the probability that a track creates a ghost hit multiplied by the track occupancy, envisaged to be around 0.6 % for the innermost barrel [7]. This yields a maximum occupancy due to ghost hits of $2 \cdot 10^{-4}$ for the non-irradiated modules, slightly smaller than the maximum noise occupancy of $5 \cdot 10^{-4}$.

7 High intensity program

In ATLAS, with a signal occupancy in the SCT of up to 1%, it is important that a module recovers fast from a track so as to be ready to respond to the

	Total Ghost Hits (%)	Due to Cross talk (%)
Non Irradiated	0.3 ± 0.1	0.3 ± 0.1
Irradiated	1.2 ± 0.3	0.8 ± 0.2

Table 5
Probability that a track creates a ghost hits for non-irradiated and irradiated detectors. The contribution of cross talk has been estimated from an analysis processing only tracks near the strip.

next. Two cases should be distinguished:

- When two tracks are close together in time, but spatially separated, switching of the comparator due to the first particle could influence the detection efficiency of the second.
- When two tracks are incident on the same strip and close together in time, the shaper pulses will most likely overlap. In edge sensing operation the second track will then not be detected. Thus, the detection of the second particle depends on the fast recovery of the front-end electronics. The specifications for the SCT front-end electronics state that the minimum L1 spacing is two bunch crossings. The double pulse resolution specification is that two 3 fC [6] signals separated by 50 ns should be detected.

The high intensity programme of this beamtest attempted to measure the effect of the high rate of beam particles on the tracking efficiency in both cases. To this end, in the last days of the beam period, the trigger logic and DAQ software were altered as previously described such that each accepted beam trigger resulted in 8 consecutive L1As being issued to the modules under test and the binary telescope modules, resulting in the reading out of the full binary information from a 600 ns time interval starting at the time of passage of the particle which caused the accepted trigger. The trigger delay was optimised so that the triggered track fell in the first clock cycle of this period. The remaining time buckets were then occupied randomly by particles following the particle which caused the accepted trigger. As the beam intensity was set high for these measurements there was a useful probability of for subsequent track occupancy. The time resolution of the binary telescope could thus be used to assign a time stamp to each of these subsequent tracks.

Figure 11 shows the distribution of the reconstructed tracks over the first 19 clock cycles for the lowest and highest beam intensities of the October beam test. For low intensity (20.000 particles/spill) the probability to find a random

[6] Note that the charge deposition in the test beam follows a Landau distribution. The median charge after charge sharing is around 3.4 fC, but much higher signals also occur.

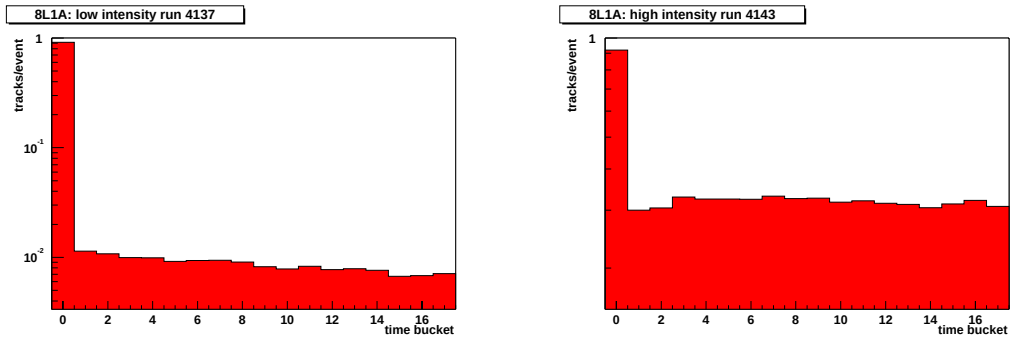

(a) (b)

Fig. 11. Distribution of reconstructed tracks for the 24 time buckets covered by the 8 L1A triggers. For low *(a)* and high *(b)* beam intensity

track in a given clock cycle is of the order of 1%, while it goes up to about 30% for the highest beam intensity in the October test beam (nearly a million particles/spill).

With the time stamp of the tracks from the binary telescope and the burst counter of the event from the DUTs, one can unambiguously assign both tracks and module hits to one of the time buckets. Within each bucket efficiency is defined in the usual way: if a DUT hit is found within 150 microns of the track position extrapolated from the telescope, the event is considered to be efficient. Figure 12 shows the efficiency versus time. There is no significant difference between the efficiency measured in the first and consecutive buckets. This indicates that the high trigger rate - and the resulting activity in the front-end - oes not affect the efficiency.

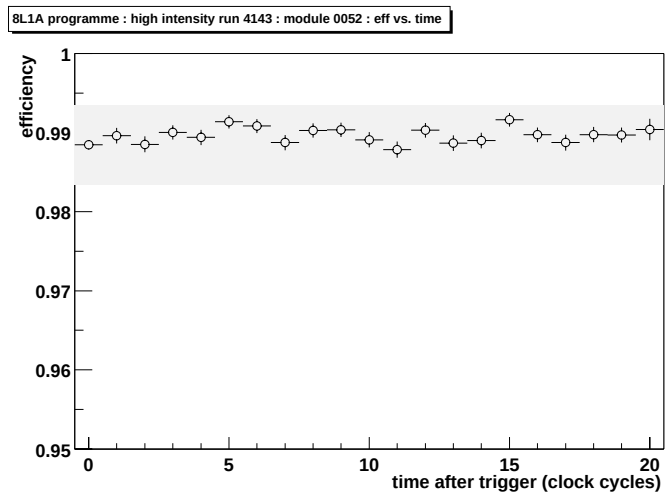

Fig. 12. Efficiency versus the time bucket counting from the scintillator trigger.

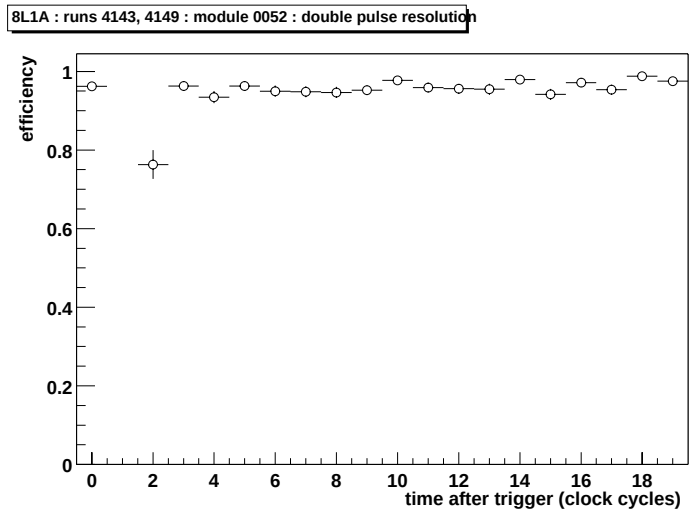

Fig. 13. Efficiency versus the time bucket counting from the accepted trigger for events where tracks coincide on the same strip.

The second case concerns tracks that are close together in time and are incident on the same strip. As the probability for this to occur is quite low, a number of high statistics - one million events - runs were taken at the highest intensity. Still, the number of tracks that satisfy the cuts is of the order of several hundreds per time bin. To study the efficiency in this case, a primary track is defined as the track corresponding to the first accepted trigger after release of the DAQ busy. This is the trigger which initiates the sequence of eight L1As. The first bin in figure 7 shows the efficiency for these primary tracks. A second track is only accepted if the strip it extrapolates to coincides with that of the primary track. Bins labeled 2 through 18 show the efficiency measured on the secundary track for different delays between both tracks. In the second bin the separation between both tracks is 25 ns. Hardly any coinciding tracks are found due to the double pulse resolution of the binary telescope modules. No efficiency measurement can be done here. For tracks 50 ns after the primary track the efficiency is significantly less than normal. For delays between both tracks of 75 ns and more full efficiency is observed.

8 Conclusion

In the beam period in October 2001, SCT prototype modules were tested in a beam with a time structure similar to that envisaged for the ATLAS experiment, with particle occupancy confined to very short time buckets synchronous with the 40MHz accelerator bunch crossing clock. The occupied time buckets

occurred in fixed length trains in a regular cycle corresponding to the 43kHz SPS beam orbit period in a manner somewhat similar to the expected LHC timing structure. The SCT DAQ was configured to provide front-end ASIC reset operation synchronous with the bunch trains in a way similar to that foreseen for operation in ATLAS. The ABCD3TA chips respond correctly to this situation.

A binary telescope, consisting of SCT modules, was used for the first time. This telescope's excellent time resolution allows to time stamp the tracks - i.e., to assign the tracks unambiguously to a certain clock cycle. The spatial resolution of the track extrapolation, approximately 17 microns, is sufficient to identify correctly the strips hit by the particle tracks in SCT modules under test.

The beamtest was divided into two periods. In the first period, data were taken at relatively low beam intensity, with readout of single events triggered by the scintillators with relatively long dead-time between accepted triggers. Measurements of the charge for different trigger delays form a cross-check to standard beam test measurements. The synchronous readout allowed a study of intricate timing effects that cannot normally be measured. The probability for a track at pependicular incidence to create ghost hit is found to be around 0.3 % and 1.2 % respectively for unirradiated and irradiated modules. At this level the occupancy in the ATLAS experiment is likely dominated by noise. The efficiency is quite robust against timing mismatches of up to 3 ns.

For the second part of the programme the beam intensity was raised to the maximum. At this rate, multiple tracks occur in each bunch train. On receipt of a scintillator trigger, 8 consecutive L1As were sent to the front-end ASICs, resulting in readout of the binary hit information from a consecutive block of 24 bunch crossings, i.e., 600 ns. The tracking efficiency is found not to be significantly affected by other tracks in this time traversing the module and leading to switching of the comparator. When both tracks coincide in the same readout strip the double-pulse resolution of the front-end comes into play. For tracks separated by 75 ns or more, no loss of efficiency was measured. The efficiency for a track hitting a readout strip 50 ns after it was hit by a previous track is observed to be reduced to around 75 %.

References

[1] A.Barr et al., Beamtests of ATLAS SCT Modules in August and October 2001, ATLAS Internal Note ATL-COM-INDET-2002-017

[2] Y.Unno et al., Beam test of non-irradiated and irradiated ATLAS SCT microstrip modules at KEK, Proceedings of the IEEE Nuclear Science

Symposium, San Diego, November 2001. Accepted for publication in Trans. Nucl. Sci.

[3] T. Akimoto et al., Beam study of irradiated ATLAS-SCT prototypes, Proceedings of the 5th Florence conference, NIM A 485 (2002) 67-72

[4] A. Barr et al., Beamtests of Prototype ATLAS SCT Modules at CERN H8 in June and August 2000, ATLAS Internal Note ATL-COM-INDET-2001-016

[5] J. Bernabeu et al., Results from the 1999 H8 beam tests of SCT prototypes, ATL-INDET-2000-004, NIM A 466 (2001) 397-405

[6] The ATLAS collaboration, ATLAS Technical Proposal, CERN/LHCC/94-43 (1993)

[7] The ATLAS collaboration, ATLAS Technical Design Report, Section Inner Detector, volume II, CERN/LHCC 97-17 (1997)

[8] The ATLAS Semiconductor Tracker (SCT), http://atlas.web.cern.ch/Atlas/GROUPS/INNER_DETECTOR/SCT

[9] S.J.M Peeters, Alignment of the ATLAS precision tracker using tracks ATL-COM-INDET-99-007

[10] Data summary files from the October 2001 beam test: /castor/cern.ch/atlas/testbeam/sct/2001/dst_bin/, /castor/cern.ch/atlas/testbeam/sct/2001/dst_8l1a/

[11] The Valencia offline web page http://alpha.ific.uv.es/sct/tb01/tb01.html

[12] J. Bernabeu et al., Measurements of the temperature dependence of the calibration and threshold DAC of the ABCD chip http://alpha.ific.uv.es/sct/activities/electronics/dactempdep/

[13] S.Gadomski, P.Reznicek, Measurement of Amplifier Pulse Shapes in SCT Modules using a laser setup. ATL-INDET-2001-010

[14] T.Akimoto et al., Characteristics of Irradiated Silicon Microstrip Detectors with $\langle 100 \rangle$ and $\langle 111 \rangle$ Substrates. NIM A466 (2001) 354-358